On The Profile Of Frequency Dependent Series Resistance And Interface States In Al/TiO_2/p-Si (MIS) Structures

İsmail Arsel[1,*]

[1]*Physics Department, Faculty of Arts and Sciences, Batman University, 72100, Batman, Turkey*

**e-mail: ismail.arsel@batman.edu.tr*

Abstract:

The frequency dependence of capacitance-voltage (*C-V*) and conductance-voltage (*G/ω-V*) characteristics of the Al/TiO_2/p-Si (MIS) structures by prepared the sol-gel method have been investigated taking into account the effect of the interface states (N_{ss}) and the series resistance (R_s) at room temperature. It is found that the measured capacitanec (*C*) and conductance (*G/ω*) are strongly dependent on bias voltage and frequency. The values of measured *C* and *G/ω* decrease in accumulation and depletion regions with increasing frequencies due to localized N_{ss} at Si/TiO_2 interface. The R_s vs. *V* plots give a peak and the peak position is shifting toward inversion region with decreasing frequency. In order to obtained the real MIS capacitance and conductance both *C-V* and *G/ω-V* measured under forward and reverse biases were corrected for the effect of R_s. Frequency dependent the *C-V* and *G/ω-V* measurements confirm that the N_{ss} and R_s of the MIS structures are very important two parameters that strongly influence the electrical characteristics.

Keywords: Sol-gel method; Al/TiO_2/p-Si (MIS) structures; Interface state density; Series resistance; Frequency dependence. MİS: Metal Insulator Semiconductor (Metal-Yalıtkan – Yarıiletken)

Özet

Sol-gel yöntemiyle hazırlanan Al/TiO_2/p-Si (MIS) yapıların iletkenlik-voltaj(*G/ω-V*) ve kapasitans-voltaj (*C-V*) karakteristiklerinin frekansa bağımlılığı oda sıcaklığında seri dirençler (R_s) ve arayüzey (N_{ss}) durumlarına etkisi gözönüne alınarak incelenmiştir. Ölçülen kapasidans (*C*) ve iletkenkiğin (*G/ω*), frekansa ve öngerilime kuvvetle bağlı olduğu bulunmuştur. Ölçülen sığa (*C)* ve iletkenlik (*G/ω)* değerlerinin, dolma ve boşalma bölgelerinde frekansın artması ile azaldığı, Si/TiO_2 arayüzeyinde N_{ss} ölçülmüştür. Seri direnç-gerilim (R_s-V), grafiğinde bir tepe noktası vardır ve tepe noktasının yeri, azalan frekansla birlikte ters bölgeye doğru kayar. Gerçek (MIS) kapasidans (*C*) ve iletkenlik (*G/ω*) değerlerini elde etmek amacıyla kapasidans-gerilim (*C-V*) ve iletkenlik-gerilim (*G/ω-V*) ölçümlerinin her ikisi ileri ve geri önyargılar altında seri dirençlerin etkisi için düzeltilmiştir. Frekansa bağlı kapasidans-gerilim (*C-V*) ve iletkenlik-gerilim (*G/ω-V*) ölçümleri son derece etkili elektriksel karakteristiklerin çok önemli iki parametresi MMS yapısında R_s ve N_{ss} olduğunu gösterir.

Anahtar Kelimeler: Sol-gel metodu; Al/TiO_2/p-Si (MIS) yapılar; Arayüzey durum yoğunluğu; Seri dirençler; Frekansa bağlılık.

1. INTRODUCTION

In metal-insulator-semiconductor (MIS) structures, metal and semiconductor remain separated by an insulating layer and there is a continious distribution of interface states (N_{ss}) at semiconductor/insulator (Si/TiO_2) interfaces. These structures constitute a kind of capacitor which stores the electric charges. There are several possible sources of error, which cause deviations from the ideal MIS behaviour, must be taken into account. These include the effects of interface states at semiconductor/insulator interface, insulator layer at metal/semiconductor interface, series resistance (R_s) of structure and formation of barrier height at metal/insulator interface. This deviations mainly takes the form of uncommonly the slope and large intercept voltage of at forward bias, and a nonlinearity of C^{-2}-V plots in the reverse bias region. When a voltage is applied across the MIS structure, the combination of insulator layer, depletion layer and series resistance of structure will share applied bias voltage. Especially both N_{ss} and R_s significantly alters the MS and MIS structure capacitance (C) and conductance (G) characteristics from their ideal behaviour and makes the measured C and G strongly frequency dependent [1-9]. At sufficiently high frequencies ($f \geq 500$ kHz), the charges at the interface states cannot follow an ac signal, but at low frequencies the charges can easily follow an ac signal and they are capable of these charges increase with decreasing frequency. Depending on the time constant, interface states may respond to an ac signal at low frequencies and contribute an excess capacitance [1,7,10]. Therefore, the frequency dependent C and G characteristics are very important in order to obtain accurated and reliable results. The characterisation of N_{ss} and R_s in MIS structure has become a subject of very intensive research and reported in the literature fore more than four decades [8-14]. In a recent work [15], the C-V characteristics of Schottky barrier diodes (SBDs) has been investigated considering the R_s effect. They investigate only the C-V plot in the high frequency limit when N_{ss} cannot follow the ac signal.

In recent year, the formation of an insulator layer on Si such as SnO_2 [16], Si_3N_4 [17], and TiO_2 [18] films are being investigated as a potential material in replecing silicon-dioxide (SiO_2). The low densities of surface states and high dielectric permitivity are the important advantage of these films acording to SiO_2. There are various of methods have been used for the preparation of TiO_2 films including sputtering [19], e-beam evaporation [20], chemical vapor deposition [21] and sol-gel process [22,23]. Among them the sol-gel method is one of the promising methods because optical and other properties of thin films can be controlled easily by changing the solution composition and deposition condition.

In this present study, we studied to investigate experimentally the frequency dependece of *C-V* and *G-V* characteristics of Al/TiO_2/p-Si MIS structures by considering the N_{ss} and R_s effects. Therefore, the electrical properties of MIS structures were investigated in the frequency range of 10 kHz-2 MHz at room temperature under both reverse and forward bias (from -4 V to 4 V). In addition, the high frequencies *C-V* and *G-V* characteristics for 700 kHz and 2 MHz were corrected for the effect of R_s to obtain the real MIS capacitance and conductance. Experimantall results show that both N_{ss} and R_s are important parameters that influence the electrical characteristics of MIS structures.

2. EXPERIMENTS

In order to prepare a TiO_2 solution, firstly 1.2 ml titanium tetraispropoxide [$Ti(OC_3H_7)_4$, Merck] was added in 15 ml ethanol [C_2H_6O, Merck] and the solution was kept in a magnetic mixture for 1 hour. Then, 5 ml glacial acetic acide [$C_2H_4O_2$, Merck] and 10 ml ethanol were added in the solution and it was mixed in the magnetic mixture for 1 hour for each additive component. As a last step, 1.5 ml trietilamine [$(S_2H_5)_3N$, Merck] was added in the solution and the final solution was subjected to the magnetic mixture for 3 hours.

A lot of metal-insulator-semiconductor (Al/TiO_2/p-Si) structures were fabricated on the 5-inch diameter float zone <111> p-type (boron-doped) single crystal silicon wafer with a thickness of 600 μm and resistivity of 5-10 Ω.cm. For the fabrication process, Si wafer was degreased through RCA cleaning procedure [24]. Then, it was subjected to the drying process in N_2 atmosphere for a prolonged time. Following the drying process, high-purity aluminium (99.999%) with a thickness of 1500 Ǻ was thermally evaporated from the tungsten filament onto the whole back surface of the Si wafer in the pressure of 10^{-7} Torr. In order to obtain a low-resistivity ohmic back contact, Si wafer was sintered at 580 ^oC for 3 minutes in N_2 atmosphere.

The dipping process was performed by help of a home-made motorized unit and each sample was dipped into the solution 3 times. After each cleaned p-type silicon crystal was dipped into the solution, one substrate of alloy formed surface of Si wafer was cleaned with ethanol. After each dipping process, samples were subjected to repeated annealing processes at temperatures of 200 ^{o}C for a five-minute period. Finally, the samples were post-annealed at temperature of 500 °C for 1 hour period.

In order to obtain a rectifying contact on the front surface of p-Si with coated TiO_2, a high-purity aluminium layer was formed on the surface in a high vacuum with the pressure of 10^{-7} Torr. The interfacial insulator layer thicknes was estimated to be about 89 Å by spectroscopic ellipsometry (VASE M2000, Woolam).

The forward and reverse bias capacitance-voltage (*C-V*) and conductance-voltage (*G-V*) measurements were performed in the frequency range of 10 kHz-2 MHz by using a HP 4192 A LF impedance analyzer (5 Hz to 13 MHz) and the test signal of 50 mV_{rms}. All measurements were carried out at the room temperature and in the dark.

3. RESULTS AND DISCUSSIONS

There are a number of suggested methods [1,25-27] which help to extract the R_s of structure, and among them the most important one is the conductance methode, developed by Nicollian and Goetzberger [1]. In this method, the frequency dependent both forward and reverse bias *C-V* and *G/ω -V* measurements give the detail information on the distribution profile of R_s of MIS structure. When the MIS structure is biased in to strong accumulation, the impadance $(Z_{ma}=1/Y_{ma})$ is given by [1]

$$Z_{ma} = \frac{1}{G_{ma} + j\omega C_{ma}} \qquad (1)$$

where C_{ma} and G_{ma} is the measured capacitance and conductance, in strong accumulation region. Series resistance is the real part of the impedance ($Z_{ma} = 1/Y_{ma}$) or:

$$R_S = \frac{G_{ma}}{G_{ma}^2 + (\omega C_{ma})^2} \qquad (2)$$

The insulator layer capacitance (C_{ox}) is obtained by substituting R_s from Eq. (2) into to relations

$$C_{ox} = C_{ma}\left[1+\left(\frac{G_{ma}}{\omega C_{ma}}\right)^2\right] = \frac{\varepsilon_i \varepsilon_0 A}{\delta} \qquad (3)$$

Thus corrected capacitance (C_c) and conductance (G_c) at the frequency of interest are:

$$C_c = \frac{\left[G_m^2 + (\omega C_m)^2\right] C_m}{a^2 + (\omega C_m)^2} \qquad (4a)$$

and

$$G_c = \frac{G_m^2 + (\omega C_m)^2 a}{a^2 + (\omega C_m)^2} \qquad (4b)$$

respectively, where $a = C_m - \left[G_m^2 + (\omega C_m)^2\right] R_S$ and C_m and G_m are the capacitance and conductance measured across the MIS structure at any bias voltage.

The capacitance-voltage-frequency (*C-V-f*) and conductance-voltage-frequency (*G/ω-V-f*) characteristics of Al/TiO_2/p-Si/Al (MIS) structure was measured in the frequency range of 10 kHz-2 MHz and are given in Figure 1(a) and (b), respectively.

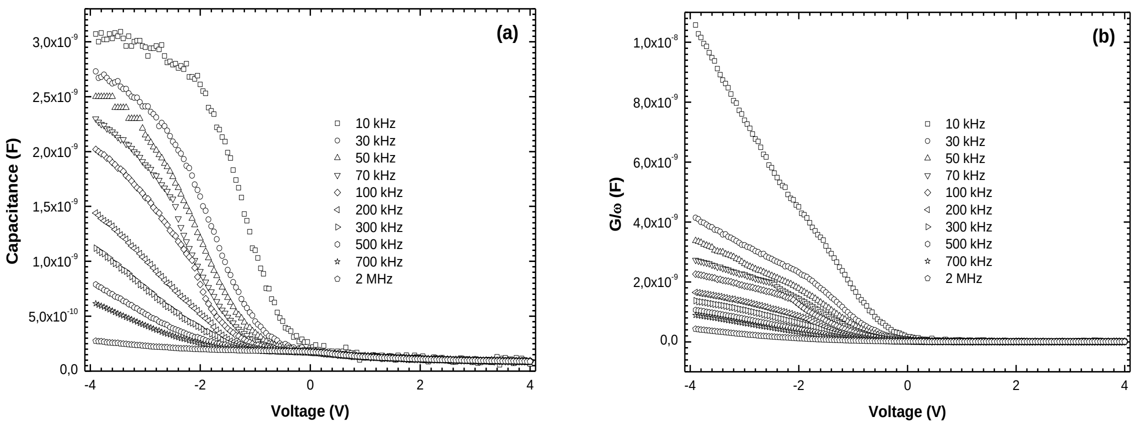

Figure 1. The frequency dependent plots of (a) the capacitance-voltage and (b) conductance-voltage characteristics of Al/TiO2/p-Si MIS structure at room temperature.

As can be seen from Figure 1(a) and (b) both curves have three distinct regimes of accumulation-depletion-inversion. The values of measured *C* and *G/ω* decrease in accumulation and depletion regions with increasing frequencies due to localized N_{ss} at Si/TiO_2 interface. Figure 2(a) and (b) shows the capacitance and conductance as a function of frequency in the voltage range of -0.5 to -3 V, with the step of 0.5 V as a parameter. As can be seen in Figure 2(a) and (b), the measured capacitance and conductance decrease with increasing frequency in the frequency range of 10 kHz to 2 MHz. Such behaviour of the *C* and *G/ω* is atributed to particial distribution of interface states at Si/TiO_2 interfaces and R_s of structure [1]. At low frequencies, the N_{ss} can easily follow the ac signal and yield an excess capacitance, which depends on frequency and time constant of interface states [1,10]. However, in sufficiently high frequency limit ($f \geq 500$ kHz), the N_{ss} can hardly follow the ac signal and the contribution of interface states capacitance to the total capacitance may be neglected. In this case, the R_s seems important parameter, which causes the *C-V* and *G/ω-V* characteristics of MIS structures to be non-ideal [6,16,28].

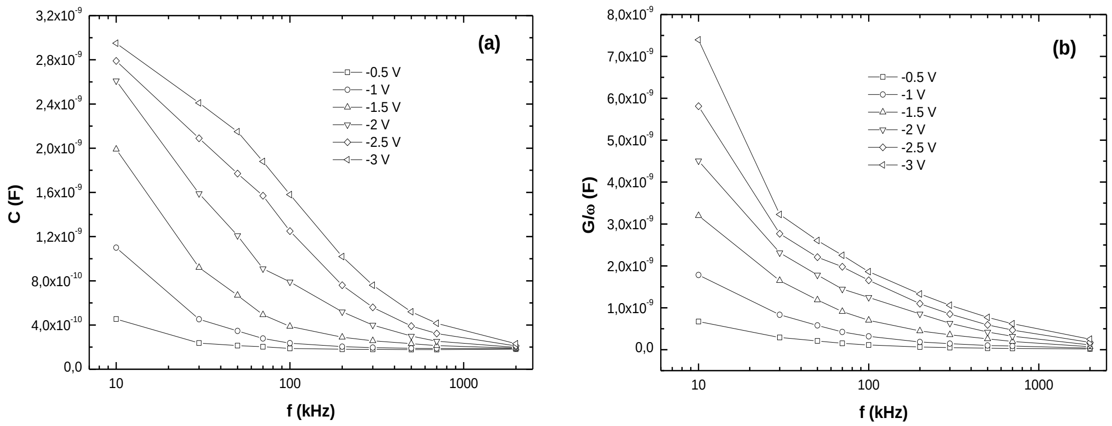

Fig. 2. (a) The capacitance-frequency and (b) conductance-frequency characteristics of Al/TiO2/p-Si MIS structure for various reverse bias at room temperature.

Using Eq. (2) the values of R_s were calculated as a function of bias in the frequency range of 100 kHz-2 MHz and are given in Figure 3. As can be clearly seen from the Figure 3, the R_s gives a peak. The peak position of R_s is shifting toward inversion region with decreasing frequency. Such behaviour of R_s is attributed to the particular distribution of localized N_{ss} at Si/TiO_2 interface states and interfacial insulator layer at Al/p-Si interface.

In order to obtained the real diode capacitance C_c and conductance G_c/ω, the capacitance of the samples at high frequency was measured under forward and reverse biases and corrected for the effect of series resistance using Eqs. (4a) and (b). When the correction was made on the *C-V* plot for the effect of series resistance, the values of the corrected C_c increased with increasing voltage, especially under reverse bias, as seen

Figure 4a. The effect of interface states can be eliminated when the *C-V* and *G/ω-V* plots are obtained at high frequency ($f \geq$ 500 kHz) [29], since N_{ss} can not follow a.c. signal. On the other hand, the plot of the corrected G_c/ω gives a peak, proving that the charge transfer can take place through the interface (Figure 4b).

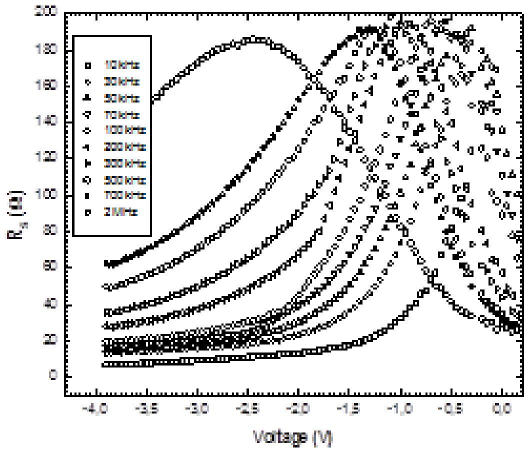

Fig. 3. The variation of the series resistance as a function of voltage for various frequencies of Al/TiO2/p-Si MIS structure at room temperature.

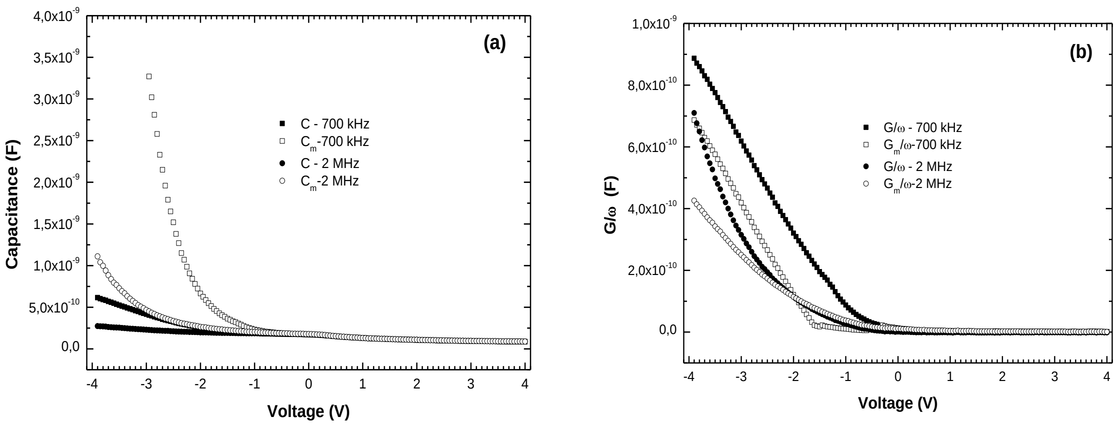

Fig. 4. The voltage dependent plot of the corrected the high frequencies (a) capacitance and (b) conductance curves at room temperature.

The density of interface states (N_{ss}) at Si/TiO_2 can be derived from Hill-Coleman method [30]. According to this method, N_{ss} is given by

$$N_{SS} = \frac{2}{qA}\frac{(G_m/\omega)_{\max}}{((G_m/\omega)_{\max} C_{ox})^2 + (1-(C_m/C_{ox}))^2} \qquad (5)$$

Where, A is the area of the structure, $(G_m/\omega)_{\max}$ is the maximum measured conductance value. Fig. 5 shows the N_{ss} decrease with increasing frequency. The high values of C and G at low frequencies were atributed to the excess capacitance resulting from the N_{ss}, which is in equilibrium with the semiconductor that follows the ac signal. As can be seen in Figure 5, the values of N_{ss} are sufficiently low and promotes the formation of low defect density interface.

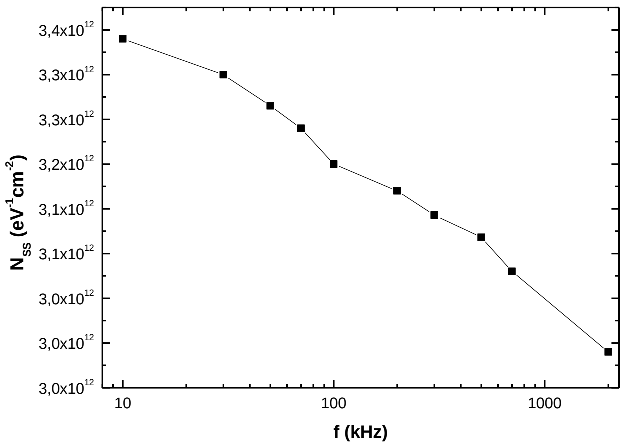

Figure 5. The variation of the N_{ss}, for the Al/TiO_2/p-Si MIS structure as a function of the frequency at room temperature.

4. CONCLUSIONS

To investigate the effects of the series resistance (R_s) and the interface states (N_{ss}) on the electrical characteristics of Al/TiO_2/p-Si (MIS) structures by using the sol-gel method, the C-V and G/ω-V characteristics have been investigated in the frequency range of 10 kHz-2 MHz. Experimental results show that the measured C and G/ω are strongly dependent on bias voltage and frequency. The values of measured C and G/ω decrease in accumulation and depletion regions with increasing frequencies due to excess capacitance resulting from the N_{ss} which is in equlibrium with the semiconductor that follows the ac signal. The effect of R_s on the C and G/ω are found noticable at high frequencies. Therefore, the values of C and G/ω were corrected for the effect of R_s both reverse and forward bias. While the corrected capacitance (C_c) value increases in accumulation and depletion region the corrected conductance (G_c/ω) value decreases according to their measured values. The R_s vs. V plot gives a peak for each frequencies, decreasing with increasing frequencies. These results show that prepared MIS structures have been controled by interfacial insulator layer and interface states, which are responsible for the non-ideal behaviour of *C-V* and *G/ω-V* characteristics.

ACKNOWLEDGMENTS

This work is supported by Turkish of Prime Ministry State Planning Organization (DPT) Project number: 2010BKV1285.

REFERENCES

[1] E H Nicollian, J R Brews, Metal-Oxide Semiconductor (MOS) Physics and Technology, Wiley, New York, 1982.

[2] S M Sze, K Ng Kwog, Physics of Semiconductor Devices,. third ed., Wiley, New York, 2007.

[3] H C Card, E H Rhoderick, *J. Phys. D* **4**, 1589 (1971).

[4] A Singh, *Solid-State Electron.* **28**, 223 (1985).

[5] P Chattopadhyay, A N Daw, *Solid-State Electron.* **29,** 555 (1986).

[6] P Chattopadhyay, B Raychaudhuri, *Solid State Electron.* **36,** 605 (1993).

[7] H Kanbur, Ş Altındal, A Tataroğlu, *Appl. Surf. Sci.* **252,** 1732 (2005).

[8] D Sands, K M Brunson, M H Tayarani-Najaran, *Semicond. Sci. Tech.* **7,** 1091 (1992).

[9] A Tataroğlu, Ş Altındal, M M Bülbül, *Microelec. Eng.* **81,** 140 (2005).

[10] J H Werner, Metallization and Metal-Semiconductor Interface, Plenum Press, New York, 1989.

[11] B R Chakraborty, N Dilawar, S Pal, D N Bose, *Thin Solid Films* **411,** 240 (2002).

[12] F Parlaktürk, Ş Altındal, A Tataroğlu, M Parlak, A Agasiev, *Microelec. Eng.* **85,** 81 (2008).

[13] S Pandey, S Kal, *Solid-State Electron.* **42,** 943 (1998).

[14] Z Ouennoughi, *Phys. Stat. Sol.* **160,** 127 (1997).

[15] P Chattopadhyay, B Raychaudhuri, *Solid-State Electron.* **35,** 875 (1992).

[16] A Tataroğlu, Ş Altındal, *Microelectron. Eng.* **83**, 582 (2006).

[17] S Zeyrek, Ş Altındal, H Yüzer, M M Bülbül, *Appl. Surf. Sci.* **252,** 2999 (2006).

[18] O Pakma, N Serin, T Serin, Ş Altındal, *J. Appl. Phys.* **104,** 014501 (2008).

[19] A Czapla, E Kusior, M Bucko, *Thin Solid Films* **182,** 15 (1989).

[20] G Sanon, R Rup, A Mansingh, *Thin Solid Films* **190,** 287 (1990).

[21] H Y Ha, S W Nam, T H Lim, I H Oh, S A Hong, *J. Membr. Sci.* **111,** 81 (1996) .

[22] J P Chatelon, C Terrier, E Bernstein, R Berjoan, J A Roger, *Thin Solid Films* **247**, 162 (1994).

[23] A Maddalena, R Dal Maschio, S Dire, A Raccanelli, *J. Non-Cyrst. Solids* **121,** 365 (1990).

[24] W Kern, Handbook of Semiconductor Cleaning Technology, Noyes, New York, 1993.

[25] H Norde, *J. Appl. Phys.* **50,** 5052 (1979).

[26] K Sato, Y Yasumura, *J. Appl. Phys.* **58,** 3655 (1985).

[27] S K Cheung, N W Cheung, *Appl. Phys. Lett.* **49,** 85 (1986).

[28] B Tataroğlu, Ş Altındal, A Tataroğlu, *Microelec. Eng.* **83**, 2021 (2006).

[29] M M Bülbül, S Zeyrek, Ş Altındal, H Yüzer, *Microelec. Eng.* **83,** 577 (2006).

[30] W A Hill, C C Coleman, *Solid-State Electron.* **23,** 987 (1980).